Implementing rectangular prism parameterization in SimPEG

EOSC 555B: Course Project

Parth Pokar
43949999
ppokar@eoas.ubc.ca

1. Introduction

Inversion of geophysical data is a crucial step in mineral exploration for identifying potential deposits. In the early stages of exploration, where swift decisions are vital, industry workflows demands swift inversion results to facilitate exploration targeting but encounter challenges due to limited expertise, computational constraints, and the need for rapid decision-making. The need for expedited (albeit not necessarily high-resolution) inversion results incorporating domain knowledge is highly desirable in guiding exploration efforts.

Conventional regularized least squares type inversion is standard practice for much of industry in part due to a lack of available open-source inversion tools that incorporate alternative inversion types. SimPEG ([3]) is one open-source python based platform that attempts to fill this gap. Currently, domain knowledge regarding the target body can be included in the form of using sparse norm regularization. While effective, they lack the ability to incorporate prior knowledge about the expected shape of the target body, limiting their accuracy and interpretability. Implementation of shape parameterization techniques into SimPEG is therefore desirable.

This project aims to implement rectangular prism shape parameterization ([2]) based on the parametric level set method ([1]). This adds to the recently implemented ellipsoidal shape parameterization in SimPEG, providing greater flexibility in representing a wider range of potential target geometries. In addition to making these implementations available to the open-source community, the parameterization techniques will help in inversion workflows combining the parameterized ellipse and rectangles parameterization with existing analytic and semi-analytic forward solutions for these shapes.

The rectangular prism implementation is tested by inverting Total Magnetic Intensity (TMI) and gravity data acquired over a simulated mineral deposit with simplified geometry. Code and scripts to re-create most of the results generated for this project are available through a Github repository at the address: `https://github.com/pokarparth/EOSC555B_Project.git`

2. Parametric Level-Set methods

Parametric level set methods have been used in geophysics to represent shapes and location of a target in some background [2]. For inverse problems, the boundary of the target is represented by the zero level-set of a function. When discretized, each point on the zero level of this function can then be evolved according to a minimization problem until the function matches the shape of the target for some misfit criterion ([4]). However, working with each point of the function greatly increases the number of parameters that need to be optimized leading to ill-conditioning of the inverse problems. Instead, the level set function can be approximated by a basis functions such as radial basis function ([1]), ([9]),([6]) or shape parameterization ([8]),([2]) for which the number of parameters may be greatly reduced. The parameterized shapes can be chosen according to the expected shape of the target - for example, a skewed Gaussian ellipsoid ([8]) or a rectangular prism ([2]).
For a general inverse problem where the forward step of the form:

$$F(\mathbf{m}) + \epsilon = \mathbf{d} \tag{1}$$

where $\mathbf{m}$ represents some model function of interest that depends on the data $\mathbf{d}$ which is mapped from the function to data space by an operator F. ϵ is the noise in the data, usually assumed to be Gaussian.
In the case where there exists one or more anomalous bodies in a background,

$$\mathbf{m}(\mathbf{x}) = \mathbf{m_0}(\mathbf{x}) + \mathbf{m_p}(\mathbf{x}) \tag{2}$$

where $\mathbf{m_0}(\mathbf{x})$ is the spatial discretization of the background model and $\mathbf{m_p}(\mathbf{x})$ is the spatial discretization for the anomalous bodies. In case of shape parameterization $\mathbf{m_p}(\mathbf{x})$ are the discretized target shapes.
The inverse problem is formulated as a minimization problem over some misfit function ϕ:

$$\min \phi\left(\mathbf{m_0}, \mathbf{m_p}\right) = ||F(\mathbf{m}) - \mathbf{d}|| + \beta(R) \tag{3}$$

where β is some weighting parameter for a regularization term R.
Now, m_p may be represented by a level set function represented by indicator function (H) which indicates whether we are inside or outside the level set domain Ω such that:

$$\mathbf{H}(\mathbf{x}) = \begin{cases} 1, & \text{for } x\epsilon\Omega \\ 0, & \text{otherwise} \end{cases}$$

Finally,

$$\mathbf{m}(\mathbf{x}) = \mathbf{m_0}(\mathbf{x}) + \mathbf{H}(\mathbf{x})\mathbf{m_p}(\mathbf{x}) \tag{4}$$

3. Implementation

3.1 Model function, m

To compute $\mathbf{m}(\mathbf{x})$, I follow the approach described by Belliveau and Haber ([2]).
m_0 is kept fixed and inversion run to optimize $\mathbf{m_p}$. The choice for $\mathbf{H}(\mathbf{x})$ primarily influences the type of shape that is being parameterized.
$\mathbf{H}$ is modified to depend on spatial vector x a set of parameters $\mathbf{p}$. For a rectangular prism, parameters

$$\mathbf{p} = [hx, hy, hz, \phi_x, \phi_y, \phi_z, c_x, c_y, c_z]$$

where h_i are the side lengths of the prism; ϕ_i are the rotation angles of the prism; c_i are the coordinates of the centres of the prism for each Cartesian direction $i = x, y, z$.
The modification of $\mathbf{H}$ is implemented as:

$$\mathbf{H}(\mathbf{x}) = \sigma_{\mathbf{x}}(\mathbf{x})\sigma_{\mathbf{y}}(\mathbf{x})\sigma_{\mathbf{z}}(\mathbf{x}) \tag{5}$$

where

$$\sigma_i(\mathbf{tau}) = \frac{1}{1 + \exp -(\tau_i + h_i)/a_i} - \frac{1}{1 + \exp -(\tau_i - h_i)/a_i}$$

for a scaling factor, a_i. The appropriate choice of this scaling factor will be discussed in the **Discussion** section.

τ is derived as follows.

For a standard rotation matrix

$$\mathbf{R} = \mathbf{R_x R_y R_z}$$

where,

$$R_x = \begin{bmatrix} 1 & 0 & 0 \\ 0 & cos(\phi_x) & -sin(\phi_x) \\ 0 & sin(\phi_x) & cos(\phi_x) \end{bmatrix}$$

$$R_y = \begin{bmatrix} cos(\phi_y) & 0 & sin(\phi_y) \\ 0 & 1 & 0 \\ -sin(\phi_x) & 0 & cos(\phi_y) \end{bmatrix}$$

$$R_z = \begin{bmatrix} cos(\phi_z) & sin(\phi_z) & 0) \\ sin(\phi_z) & cos(\phi_z) & 0 \\ 0 & 0 & 1 \end{bmatrix}$$

$$\tau = \mathbf{x} - \mathbf{x_0}^T R$$

The above equations describe the implementation for one prism. For the case of n_p number of prisms, 4 can be modified as ([2]):

$$\mathbf{m}(\mathbf{x}) = \mathbf{m_0}(\mathbf{x}) + w(\mathbf{x}) \sum_{i=1}^{n_p} \mathbf{H}(\mathbf{x})\mathbf{m_p}(\mathbf{x}) \tag{6}$$

where, w is a normalization factor defined as:

$$w(\mathbf{x}) = \min\left(1, \frac{1}{\sum_{i=1}^{n_p} \mathbf{H}(\mathbf{x})}\right)$$

3.2 Testing the implementation

This section describes how the implementation of rectangular prism parameterization with equation 6 was tested using two test inversions.

The initial evaluation involved testing the rectangular prism parameterization using synthetic potential field datasets. Synthetic total magnetic intensity (TMI) data was generated for the primary test, employing an 80-point survey with a 10m spacing. The dataset was simulated over a 3D rectangular mesh with core dimensions of 800m in X and Y Cartesian directions and 500m in the Z Cartesian direction. The minimum cell size in the mesh was set to 25m to optimize computational efficiency. The data density in this simulation is deliberately an order of magnitude sparser than in typical production surveys, a computational cost consideration for this specific inversion.

The TMI data was generated based on a model (figure 1) featuring a flat rectangular block with susceptibility $m_p = 0.1$ SI embedded in a uniform background susceptibility, $m_0 = 0.0001$ SI. The block's dimensions are detailed in the table in Figure 3. To mimic realistic conditions, noise equivalent to 2% of the maximum amplitude anomaly was introduced to the simulated data prior to inversion.

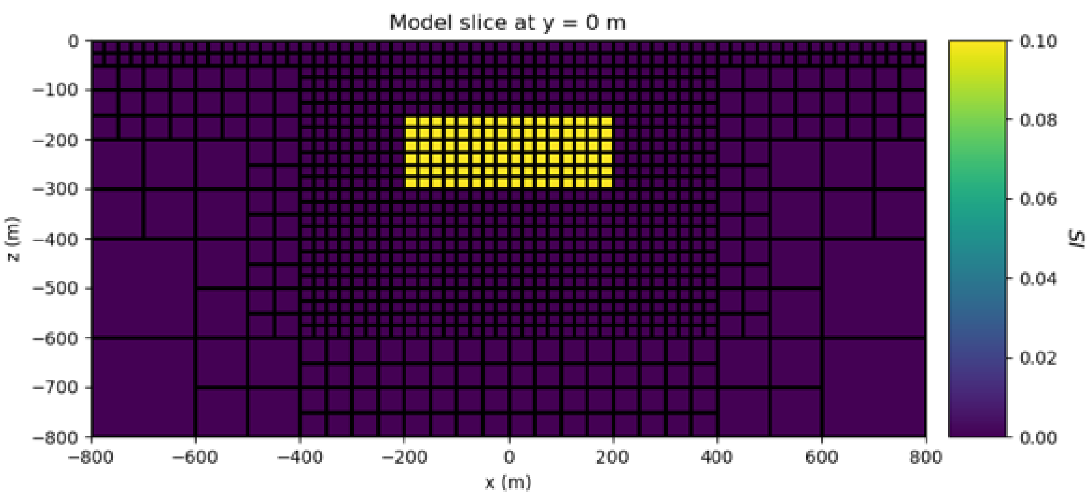

Figure 1: *True model setup used to generated synthetic TMI data*

To assess the robustness of the parameterization implementation in scenarios with multiple objects and distinct physics, a secondary test was conducted. This test model incorporated one rectangular and one spherical object as inversion targets (figure 2). Synthetic gravity data was generated for this case, utilizing a sparser mesh due to time and computational constraints.

For both inversion tests, optimization was executed using a Projected Gauss-Newton Conjugate Gradient method. Upper and lower bounds for the parameters were also imposed. Additional details can be found in the code available in the GitHub repository for this project.

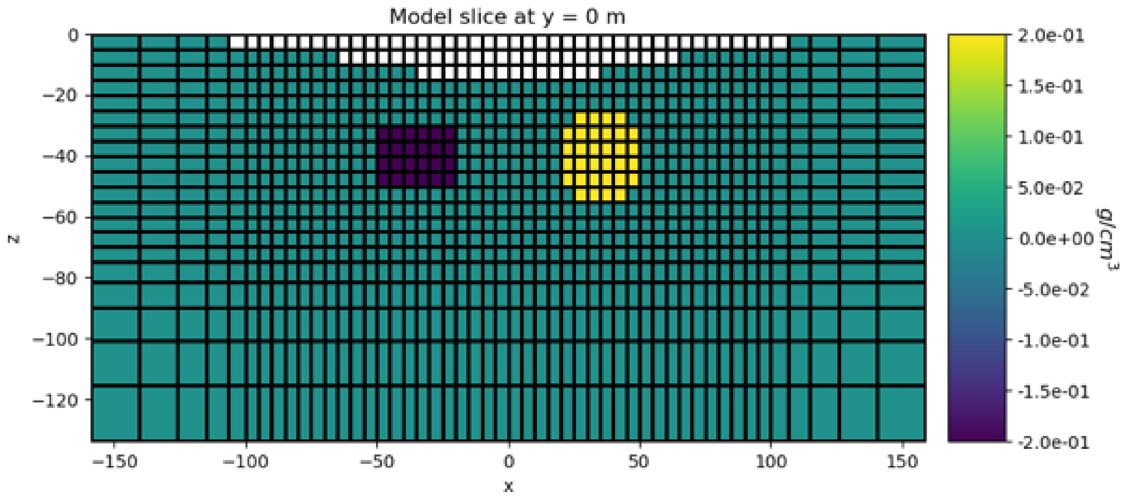

Figure 2: *True model setup used to generate synthetic gravity data.*

Side length (dx)	400	Side length (dx)	200
Side length (dy)	200	Side length (dy)	100
Side length (dz)	150	Side length (dz)	100
Dip angle (ϕ_x)	0	Dip angle (ϕ_x)	0
Dip angle (ϕ_y)	0	Dip angle (ϕ_y)	15
Dip angle (ϕ_z)	0	Dip angle (ϕ_z)	0
Centre (c_x)	0	Centre (c_x)	0
Centre (c_y)	0	Centre (c_y)	0
Centre (c_z)	-225	Centre (c_z)	-300

Figure 3: *Comparison of the parameters for the rectangular prism used to generate the true (left) synthetic TMI data and as the initial model (right) for TMI inversion.*

4. Results

Figures 4 and 5 shows the results from least squares and parametric inversion for TMI respectively. Figure 6 shows the results from the inversion of gravity data.

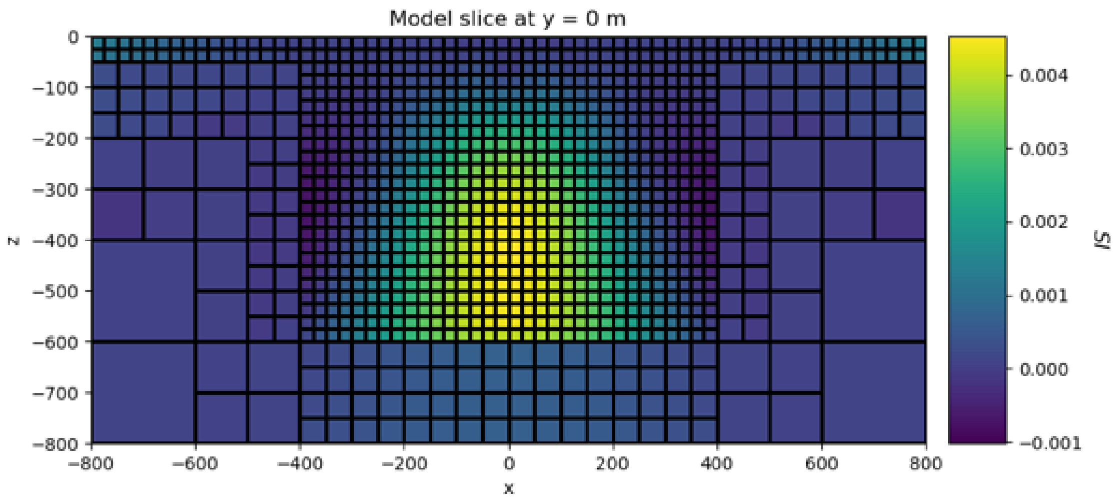

Figure 4: *Regularized least squares inversion results of TMI data*

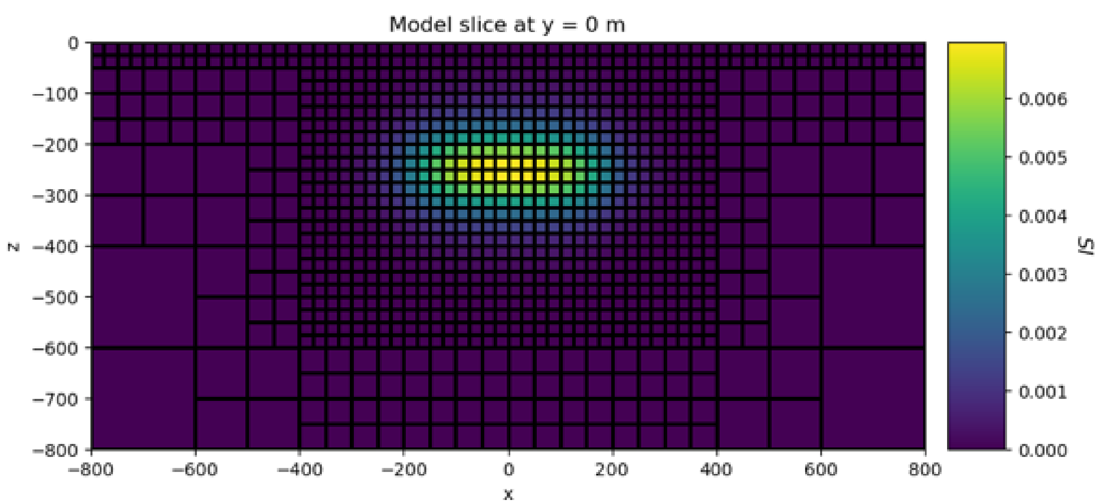

Figure 5: *Rectangular prism parametric inversion of TMI data*

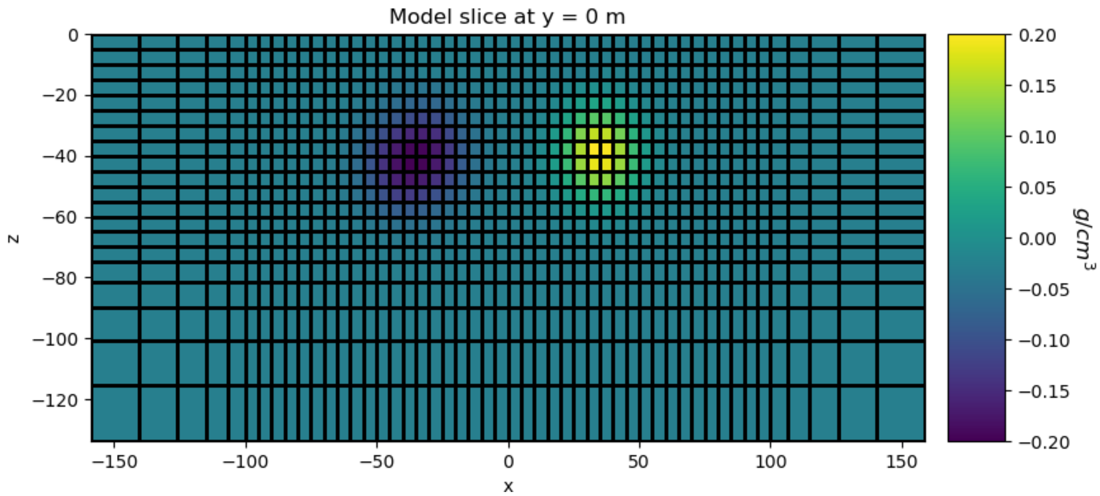

Figure 6: *Results from parametric inversion of gravity data with multiple objects.*

5. Discussion

Results from the testing show that the implementation for rectangular prism is able to successfully recover the initial model and outperforms conventional regularized least squares inversion routines.

The choice of the scaling factor in the Heaviside function is crucial to ensure Gauss Newton optimization converges. Larger values for the scaling factor make the transition at the interface of the parameterized prism less sharp. Empirical testing suggests that scaling factor should be at least twice the minimum mesh cell size to ensure convergence. (figure 7,8). One way to reduce the diffusive boundaries of the level-set function observed for larger scaling factors is to adopt a hybrid inversion approach wherein the scaling factor may be added as another parameter following a few Conjugate Gradient iterations. This allows the inversion to leverage the larger scaling factor and take larger optimization steps in the initial iterations while also ensuring that the optimization does not get stuck in to local minima for latter iterations.

The implementation successfully resolved multiple objects, achieving proper resolution of spatial extents and physical property contrast. However, the prism parameterization faced challenges in accurately resolving the shape of a sphere. Additional testing involving datasets featuring exaggerated ellipsoids revealed the limitation in the prism parameterization's ability to successfully capture the shape.

Preliminary testing involved combining both the pre-existing ellipsoidal parameterization and the prism parameterization for this dataset. This hybrid approach proved successful in simultaneously resolving the shapes and physical properties of both geometries. Future work will expand to include different physics, such as electromagnetics, to test the robustness of the method.

The preliminary implementation did not incorporate additional explicit regularization. This decision was based on the understanding that parametric level-set methods inherently impose implicit regularization by constraining the total number of parameters in the inverse problem ([8]). While the benefits of additional regularization remain unclear, future work will investigate its potential advantages.

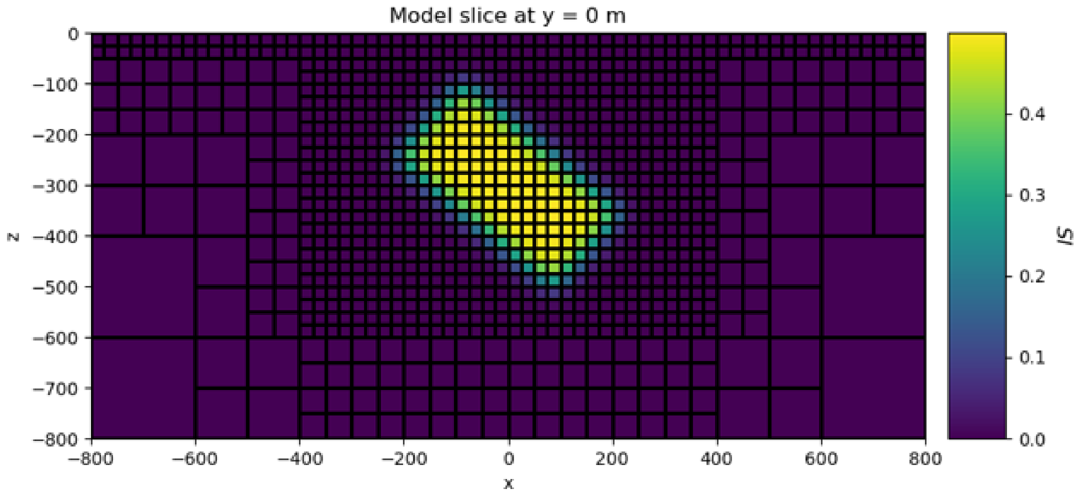

Figure 7: *Initial model for the parametric inversion with a scaling factor equal to half the minimum mesh cell size. Inversion with this initial model failed to converge.*

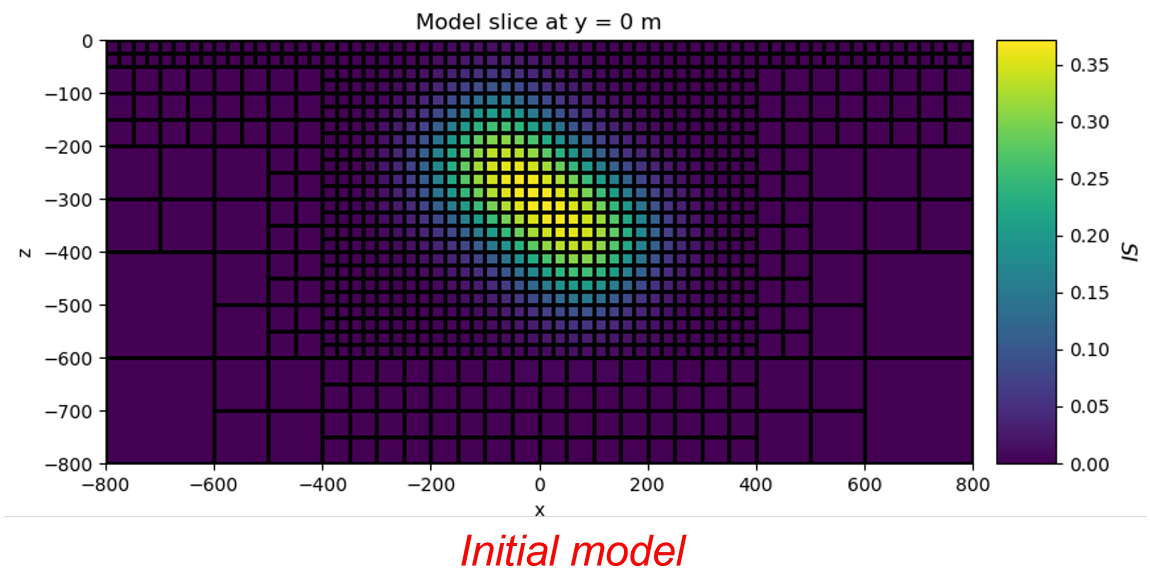

Figure 8: *Initial model for the parametric inversion with a scaling factor equal to twice the minimum mesh cell size. Inversion with this initial model successfully converged.*

Several existing implementations of parametric level-set methods utilize Radial Basis Functions (RBFs) instead of shape parameterization ([1], [6], [9]). RBFs offer greater flexibility in representing arbitrary shapes. A preliminary implementation of an RBF parameterization for SimPEG is currently underway and will be a primary focus of follow-up work.

6. Conclusion

As part of this project, implementation of rectangular prism parameterization within SimPEG was completed successfully. Implementations for multiple bodies involving any combination of prism and ellipsoidal shapes are now possible. The implementation was tested with realistic magnetic inversions as well as gravity data inversion.

The scaling factor in the Heaviside function critically influences the convergence of Gauss-Newton optimization. Empirical testing establishes that a scaling factor at least twice the minimum mesh cell size is vital for convergence. Proper choice of the scaling factor may be made using a hybrid inversion approach introducing the scaling factor as an additional parameter after a few Conjugate Gradient iterations.

While successful in resolving multiple rectangular objects and demonstrating adept spatial and property contrast resolution, the prism parameterization faced challenges in accurately representing spherical shapes.

Future investigations will expand to include different physics, such as electromagnetics, to assess the method's robustness across diverse geophysical scenarios. Explicit regularization, initially overlooked, will be explored for its potential benefits despite the implicit regularization effect of parametric level-set methods. While shape parameterization using rectangular prisms showed effectiveness in specific scenarios, preliminary implementation of RBF parameterization offering greater flexibility in representing arbitrary shapes is underway.

References

[1] Aghasi, Alireza, Misha Kilmer, and Eric L. Miller. 2011. 'Parametric Level Set Methods for Inverse Problems' *SIAM Journal on Imaging Sciences* 4 (2): 618–50. doi: 10.1137/100800208.

[2] Belliveau, Patrick, and Eldad Haber. 2023. 'Parametric Level-Set Inverse Problems with Stochastic Background Estimation'. *Inverse Problems* 39 (7). doi: 10.1088/1361-6420/acd413.

[3] Cockett, Rowan, Seogi Kang, Lindsey J. Heagy, Adam Pidlisecky, and Douglas W. Oldenburg. 2015. 'SimPEG: An Open Source Framework for Simulation and Gradient Based Parameter Estimation in Geophysical Applications.' *Computers and Geosciences*, September 2015. doi:10.1016/j.cageo.2015.09.015.

[4] Dorn, Oliver, Eric L. Miller, and Carey M. Rappaport. 2000. 'A Shape Reconstruction Method for Electromagnetic Tomography Using Adjoint Fields and Level Sets'. *Inverse Problems* 16 (5): Pages: 1119. doi: 10.1088/0266-5611/16/5/303.

[5] Heagy, Lindsey J., Rowan Cockett, Seogi Kang, Gudni K. Rosenkjaer, and Douglas W. Oldenburg. 2017. "A Framework for Simulation and Inversion in Electromagnetics." *Computers & Geosciences* 107 (October). Pages: 1–19. doi: 10.1016/j.cageo.2017.06.018.

[6] Kadu, Ajinkya, Tristan van Leeuwen, and Wim A. Mulder. 2017. 'Salt Reconstruction in Full Waveform Inversion with a Parametric Level-Set Method'. *IEEE Transactions on Computational Imaging* 3 (2). Pages: 305–15. doi: 10.1109/TCI.2016.2640761.

[7] Liu, Hui, Ye Tian, Hongming Zong, Qingping Ma, Michael Yu Wang, and Liang Zhang. 2019. 'Fully Parallel Level Set Method for Large-Scale Structural Topology Optimization'. *Computers & Structures* 221 (September). Pages: 13–27. doi: 10.1016/j.compstruc.2019.05.010.

[8] McMillan, Michael S. G. 2017. 'Cooperative and Parametric Strategies for 3D Electromagnetic Inversion'. Ph.D Thesis University of British Columbia. doi: 10.14288/1.0343483.

[9] Ozsar, Ege, Misha Kilmer, Eric Miller, Eric de Sturler, and Arvind Saibaba. 2022. 'Parametric Level-Sets Enhanced To Improve Reconstruction (PaLEnTIR)'. *Preprint arXiv.* http://arxiv.org/abs/2204.09815.